Magnetic Impurity in the two-dimensional Heisenberg Antiferromagnet

V.N. Kotov, J. Oitmaa, and O. Sushkov

School of Physics, University of New South Wales, Sydney 2052, Australia

The two-dimensional Heisenberg model at zero temperature with a quantum S=1/2 impurity spin, coupled to one site, is studied. The ground state properties of the model are calculated for large coupling, in order to study the impurity - host spin local singlet formation and related local suppression of the magnetization in the host lattice. Analytic results are obtained by developing perturbation theory around the exactly solvable two-body (impurity plus neighbor) problem and compared with results obtained by exact diagonalization of small clusters. We find that perfect screening of the impurity is only achieved for infinitely large interaction, while at intermediate coupling the local magnetization is suppressed, but non-zero.

PACS numbers: 75.10.Jm, 75.30.Hx, 75.50.Ee

I. INTRODUCTION

The problem of magnetic impurities interacting with a system of strongly correlated electrons has attracted a lot of interest recently, mainly due to the experimental discoveries of the high-T_c superconductors and new heavy fermion compounds. In the field of the high-T_c materials, the parent compounds are known to be two-dimensional (2D) antiferromagnetic (AFM) Mott-Hubbard insulators which are driven to a superconducting state by doping (e.g. with holes)[1,2]. Even though the holes can hop, thus destroying the AFM long-range order (LRO) and causing the development of superconducting pairing, the extreme limit of static holes is also believed to have physical relevance. More generally, the effect of local perturbations on the AFM order is an interesting problem by itself. Several problems in 2D have been studied - static vacancy (missing site)[3], an impurity spin with an on-site[4] and sublattice symmetric[5,6] coupling, as well as an isolated ferromagnetic bond[7,6]. Impurity spins, coupled to 1D antiferromagnets have also been considered, by applying bosonization techniques[8].

From the perspective of the heavy fermion physics, in light of some recent experimental observations, it is important to take into account strong correlations between the conduction electrons, interacting with an on-site magnetic impurity. As a starting point, a model at half filling, with a large Hubbard on-site repulsion, leading to the freezing of the conduction degrees of freedom, has been proposed[9]. The problem reduces to an impurity spin, coupled to a Heisenberg antiferromagnet. In 2D, for $T = 0$ the problem has been studied by using the linear spin-wave approximation (LSWA)[9]. For $T \neq 0$, when LRO is absent in 2D, the Schwinger boson mean-field theory was applied[10]. Also, the one-dimensional version of the problem has been studied numerically as a toy model[11,12].

In the present work we consider a magnetic impurity, coupled via an on-site Kondo coupling to a 2D quantum Heisenberg antiferromagnet at $T = 0$. Our main goal is the investigation of the interplay between LRO and local screening of the impurity spin (Kondo effect). Since LRO is present in 2D, with a staggered moment reduced to about 61 % from

its classical value, the Kondo coupling, necessary to induce considerable impurity screening is rather large. Previous works have used the LSWA with subsequent perturbation theory in the Kondo interaction[9,10] - an approach not suitable for the study of strong interactions. To get insight into the strong-coupling regime, we observe that due to the local character of the perturbation it is sufficient first to diagonalize exactly the two-body system, consisting of the impurity and directly coupled substrate spin, and then treat the remaining interaction with the AFM environment in perturbation theory. Technically we work with a two-particle Green's function which we use to construct the ground state of the system. The rest of the paper is organized as follows. Our approach is described in Section II. We also compare our analytical results with results obtained from exact diagonalization studies. The numerical procedure is outlined in Section III. Section IV contains summary of our results and discussion.

II. IMPURITY SPIN IN THE HEISENBERG ANTIFERROMAGNET.

Consider the two-dimensional spin-1/2 Heisenberg model at zero temperature with a single, spin-1/2 magnetic impurity:

$$H = J \sum_{<i,j>} \vec{S}_i.\vec{S}_j + K\vec{S}_0.\vec{\sigma} \tag{1}$$

All the couplings are antiferromagnetic $J > 0, K > 0$. We set $J = 1$ from now on. In the first term in (1) the summation is over nearest neighbors on a square lattice. The second term represents an S=1/2 spin $\vec{\sigma}$ coupled to the site $i = 0$ of the host lattice via the Kondo coupling K. It is known[1] that for $K = 0$ there is LRO in the ground state of H and the staggered magnetic moment $m \equiv < S_i^z >= 0.303$. The Kondo interaction favors singlet formation and thus suppresses the magnetization locally, leading also to screening of the impurity spin.

In order to treat the strong coupling case $K > 1$ we start by rewriting the Hamiltonian as

$$H = H_{sw} + \left\{ K\vec{S}_0.\vec{\sigma} + S_0^z \sum_{i=1}^{4} S_i^z \right\} + \left\{ \frac{1}{2} S_0^+ \sum_{i=1}^{4} S_i^- + \text{ h.c.} \right\}, \tag{2}$$

$$H_{sw} = \sum_{\mathbf{k}} \varepsilon_{\mathbf{k}} (\alpha_{\mathbf{k}}^\dagger \alpha_{\mathbf{k}} + \beta_{\mathbf{k}}^\dagger \beta_{\mathbf{k}}). \tag{3}$$

The spins $\vec{S}_i, i = 1-4$ are the nearest neighbors of $\vec{S}_0$ (see Fig.1.) and are assumed to belong to sublattice B (spin down). Here $\beta_{\mathbf{k}}$ and $\alpha_{\mathbf{k}}$ are the usual spin-wave operators with dispersion[1]:

$$\varepsilon_{\mathbf{k}} = 2\sqrt{1-\gamma_{\mathbf{k}}^2}, \ \gamma_{\mathbf{k}} = \frac{1}{2}(\cos(k_x) + \cos(k_y)). \tag{4}$$

In (2) we have explicitly separated the host spin-impurity and host spin-AFM background interaction. We have assumed that the exclusion of one spin (the one at $i = 0$) does not influence the spin-wave Hamiltonian. This is valid in the one-loop approximation (see below) which we use in the present work. However, if one wants to go beyond the lowest order (i.e. to higher loops), the influence of the $i = 0$ perturbation on the spin-wave spectrum has to be taken into account.

Since the impurity spin disturbs the AFM background only locally, we can make the mean-field substitution $S_0^z S_i^z \to S_0^z < S_i^z >= S_0^z m$. The terms in the first curly brackets in (2) then can be diagonalized exactly, while the ones in the second curly brackets will be treated as a perturbation. For the spins $\vec{S}_0$ and $\vec{\sigma}$ we introduce the fermionic representation:

$$S_0^+ = \Psi_\uparrow^\dagger \Psi_\downarrow, \quad S_0^z = \frac{1}{2}(\Psi_\uparrow^\dagger \Psi_\uparrow - \Psi_\downarrow^\dagger \Psi_\downarrow), \tag{5}$$

where $\Psi_\uparrow^\dagger$ and $\Psi_\downarrow^\dagger$ create (acting on their common vacuum) a S_0^z component $1/2$ and $-1/2$ respectively. In order for the two fermions to represent a spin-1/2 operator, they have to satisfy the constraint: $\Psi_\uparrow^\dagger \Psi_\uparrow + \Psi_\downarrow^\dagger \Psi_\downarrow = 1$, i.e. the physical states have only one fermion. The operators representing $\vec{\sigma}$ via a formula identical to (5) are denoted by $\Phi_\uparrow, \Phi_\downarrow$. Using this representation and the usual spin wave expansion for the spins $\vec{S}_i, i = 1-4$, the Hamiltonian becomes:

$$H = H_{sw} + H_0 + H_{int}, \tag{6}$$

$$H_0 = 2m(\Psi_\downarrow^\dagger\Psi_\downarrow - \Psi_\uparrow^\dagger\Psi_\uparrow) + \frac{K}{4}(\Psi_\uparrow^\dagger\Psi_\uparrow - \Psi_\downarrow^\dagger\Psi_\downarrow)(\Phi_\uparrow^\dagger\Phi_\uparrow - \Phi_\downarrow^\dagger\Phi_\downarrow) + \frac{K}{2}(\Psi_\uparrow^\dagger\Psi_\downarrow\Phi_\downarrow^\dagger\Phi_\uparrow + \text{h.c.}), \quad (7)$$

$$H_{int} = \sqrt{\frac{8}{N}}\Psi_\uparrow^\dagger\Psi_\downarrow \sum_{\mathbf{k}} \gamma_{\mathbf{k}}(u_{\mathbf{k}}\beta_{\mathbf{k}} + v_{\mathbf{k}}\alpha_{-\mathbf{k}}^\dagger) + \text{ h.c.}, \quad (8)$$

where N is the total number of lattice sites, and $u_{\mathbf{k}} = \sqrt{\frac{1}{2} + \frac{1}{\varepsilon_{\mathbf{k}}}}$, $v_{\mathbf{k}} = -\text{sign}(\gamma_{\mathbf{k}})\sqrt{-\frac{1}{2} + \frac{1}{\varepsilon_{\mathbf{k}}}}$ are the parameters of the Bogoliubov transformation. The $\mathbf{k}$ sums in (8) as well as all future formulas are over half of the first Brillouin zone, $0 < k_x, k_y < \pi$.

We have previously applied an approach, similar to the one that leads to the effective Hamiltonian (6), to study locally frustrating defects in quantum antiferromagnets[6]. The following treatment is also closely related to the one used by us in Ref.[6].

In order to diagonalize H_0 it is convenient to define the two-particle matrix Green's function $\hat{G}_{\mu\nu}$:

$$\hat{G}_{\mu\nu}(t) = -i \begin{pmatrix} < T(\Psi_\uparrow(t)\Phi_\downarrow(t)\Psi_\uparrow^\dagger(0)\Phi_\downarrow^\dagger(0)) > & < T(\Psi_\uparrow(t)\Phi_\downarrow(t)\Psi_\downarrow^\dagger(0)\Phi_\uparrow^\dagger(0)) > \\ < T(\Psi_\downarrow(t)\Phi_\uparrow(t)\Psi_\uparrow^\dagger(0)\Phi_\downarrow^\dagger(0)) > & < T(\Psi_\downarrow(t)\Phi_\uparrow(t)\Psi_\downarrow^\dagger(0)\Phi_\uparrow^\dagger(0)) > \end{pmatrix}. \quad (9)$$

As (9) suggests, the diagonal elements (11 and 22) correspond to the two-particle states $|1> \equiv |\uparrow\downarrow>$ and $|2> \equiv |\downarrow\uparrow>$, respectively, where the first arrow represents the spin $\vec{S}_0$ and the second one - the spin $\vec{\sigma}$, or, equivalently $|\uparrow\downarrow> = \Psi_\uparrow^\dagger\Phi_\downarrow^\dagger|0>, |\downarrow\uparrow> = \Psi_\downarrow^\dagger\Phi_\uparrow^\dagger|0>$, where $|0>$ is the fermionic vacuum. The off-diagonal components represent transitions between these two states. For future purposes we define also the states: $|3> \equiv |\uparrow\uparrow>$ and $|4> \equiv |\downarrow\downarrow>$. The unperturbed Green's functions (corresponding to H_0) are:

$$G_{11,22}(\omega) = \frac{1}{\omega + K/4 \pm 2m + i\delta}, \quad G_{12}(\omega) = G_{21}(\omega) = \frac{1}{\omega - K/2 + i\delta}. \quad (10)$$

Next, we evaluate the self-energy corrections to (10) to lowest, one-loop order in perturbation theory with respect to H_{int}. Evaluating the diagram of Fig.2a, we obtain:

$$\Sigma_{11}(\varepsilon) = i\frac{8}{N}\sum_{\mathbf{k}} \gamma_{\mathbf{k}}^2 u_{\mathbf{k}}^2 \int D(\mathbf{k}, \varepsilon')G_4(\varepsilon - \varepsilon')\frac{d\varepsilon'}{2\pi} = \frac{8}{N}\sum_{\mathbf{k}} \frac{\gamma_{\mathbf{k}}^2 u_{\mathbf{k}}^2}{\varepsilon - K/4 - 2m - \varepsilon_{\mathbf{k}}}. \quad (11)$$

Here $D^{-1}(\mathbf{k}, \omega) = \omega - \varepsilon_{\mathbf{k}}$ is the spin-wave Green's function, and $G_4^{-1}(\omega) = \omega - K/4 - 2m$ corresponds to the two-particle state $|4>$. Analogous calculation gives (see Fig.2b):

$$\Sigma_{22}(\varepsilon) = \frac{8}{N}\sum_{\mathbf{k}} \frac{\gamma_{\mathbf{k}}^2 v_{\mathbf{k}}^2}{\varepsilon - K/4 + 2m - \varepsilon_{\mathbf{k}}}, \tag{12}$$

and $\Sigma_{12} = \Sigma_{21} = 0$. Higher loop corrections to the self-energy can also be taken into account. Let us mention that vertex corrections do not exist due to spin conservation (reflected by the structure of the interaction (8)). The only remaining diagrams are the "rainbow" ones[13]. We find that their contribution is small compared to the dominant one of Eq.(11) and Eq.(12). Thus we restrict ourselves to the one-loop order.

Since the z component of the total spin is conserved, the wave function of the spins S_0 and σ is spanned by the states $|1>$ and $|2>$, corresponding to $S_0^z + \sigma^z = 0$. The equation for the effective energy level ε^* is:

$$\begin{vmatrix} \varepsilon^* + K/4 + 2m - \Sigma_{11}(\varepsilon^*) & K/2 \\ K/2 & \varepsilon^* + K/4 - 2m - \Sigma_{22}(\varepsilon^*) \end{vmatrix} = 0. \tag{13}$$

The correct normalized eigenstate is of the form $|12> = \mu_1|1> + \mu_2|2>$, where (μ_1, μ_2) is an eigenvector of the matrix in (13), and $\mu_1^2 + \mu_2^2 = 1$. The ground state wave function of the two-particle - spin-wave system can be written as

$$|G> = \sqrt{Z}|12>|\mathrm{sw}> + \sum_{\mathbf{k}} B_{\mathbf{k}}|\downarrow\downarrow>\beta_{\mathbf{k}}^\dagger|\mathrm{sw}> + \sum_{\mathbf{k}} A_{\mathbf{k}}|\uparrow\uparrow>\alpha_{\mathbf{k}}^\dagger|\mathrm{sw}> . \tag{14}$$

We have defined:

$$B_{\mathbf{k}} = \sqrt{\frac{8}{N}}\frac{\mu_1\gamma_{\mathbf{k}}u_{\mathbf{k}}}{\varepsilon^* - K/4 - 2m - \varepsilon_{\mathbf{k}}}, A_{\mathbf{k}} = \sqrt{\frac{8}{N}}\frac{\mu_2\gamma_{\mathbf{k}}v_{\mathbf{k}}}{\varepsilon^* - K/4 + 2m - \varepsilon_{\mathbf{k}}}, \tag{15}$$

and $|\mathrm{sw}>$ is the spin-wave vacuum, i.e. $\alpha_{\mathbf{k}}|\mathrm{sw}> = \beta_{\mathbf{k}}|\mathrm{sw}> = 0$. The first term in (14) is the coherent part of the wave function while the rest is the contribution of the intermediate states. The normalization factor Z is defined as:

$$Z = 1 + \mu_1^2\left(\frac{\partial\Sigma_{11}}{\partial\varepsilon}\right)_{\varepsilon=\varepsilon^*} + \mu_2^2\left(\frac{\partial\Sigma_{22}}{\partial\varepsilon}\right)_{\varepsilon=\varepsilon^*}. \tag{16}$$

The average of any spin operator in the state $|G>$ can be computed by using the explicit form (14). The results for the magnetization of the impurity spin and its neighbor as well as their spin-spin correlation function are:

$$M(0) \equiv < S_0^z > = \frac{\mu_1^2 - \mu_2^2}{2} Z + \frac{1}{2} \sum_{\mathbf{k}} \left(A_{\mathbf{k}}^2 - B_{\mathbf{k}}^2 \right), \tag{17}$$

$$M(\sigma) \equiv < \sigma^z > = \frac{\mu_2^2 - \mu_1^2}{2} Z + \frac{1}{2} \sum_{\mathbf{k}} \left(A_{\mathbf{k}}^2 - B_{\mathbf{k}}^2 \right), \tag{18}$$

$$C(\sigma, 0) \equiv < \vec{\sigma}.\vec{S}_0 > = \frac{1 - 2Z}{4} + \mu_1 \mu_2 Z. \tag{19}$$

In order to find the spin-spin correlation between the host spin $\vec{S}_0$ and its nearest neighbor $\vec{S}_1$ of the host lattice (see Fig.1), we need to find how $\vec{S}_1$ acts on the spin-wave states $|\mathrm{sw}>, \alpha_{\mathbf{k}}^\dagger|\mathrm{sw}>, \beta_{\mathbf{k}}^\dagger|\mathrm{sw}>$, which appear in $|G>$. This is accomplished by using the Holstein-Primakoff representation $S_1^z = -1/2 + b_1^\dagger b_1, S_1^+ = b_1^\dagger$, and performing the Bogoliubov transformation $b_{\mathbf{k}} = u_{\mathbf{k}} \beta_{\mathbf{k}} + v_{\mathbf{k}} \alpha_{-\mathbf{k}}^\dagger$. The final result is

$$C(1,0) \equiv < \vec{S}_1.\vec{S}_0 > = < S_0^z > \left\{ -\frac{1}{2} + \frac{2}{N} \sum_{\mathbf{k}} v_{\mathbf{k}}^2 \right\} + \frac{1}{2} \left[\mu_1^2 \sqrt{Z} \Sigma_{11} + \mu_2^2 \sqrt{Z} \Sigma_{22} \right]. \tag{20}$$

In Eq.(20) the self-energies are evaluated at $\varepsilon = \varepsilon^*$. The expression in the curly brackets is the LSWA magnetization $m = 0.303$. In order to compute (17-20) all the lattice sums as well as the solution of Eq.(13) have to be calculated numerically. The results are summarized in Figures 3 and 4.

Notice that in the approximation we have adopted for the Hamiltonian Eq.(6), the magnetization of the spins 1,2,3,4 (see Fig.1) is $m = 0.303$ (since they are part of the spin-wave background), and does not depend on K. In order to calculate, e.g. $< S_1^z >$ more accurately, one needs to diagonalize exactly the system of three spins S_0, S_1, σ and treat all the rest of the spins in the linear spin-wave approximation. Conceptually the calculation is very similar to the one presented above. However, since the technical details are more involved and not particularly illuminating, we do not describe them here[14]. The results for $< S_1^z >$ are given in Table.I. The diagonalization of the three-body system is expected to produce also more accurate results for $C(1,0)$. We have found, however, that the difference between the three-body calculation and Eq.(20) is numerically very small.

In our technique the magnetization of the unperturbed Heisenberg antiferromagnet ($K = 0$) differs from the LSWA value $m = 0.303$ and depends on the size of the "cluster" - the number of spins that are exactly diagonalized. We find the magnetization to be 0.272 if the cluster consists of one spin ($M(0)$ from Fig.3.) and 0.318 for a cluster of two spins ($< S_1^z > (GF)$ from Table.I). We generally expect that the accuracy of our method will increase as the size of the cluster increases and higher orders of perturbation theory in the cluster-AFM background interaction are taken into account.

The results for the magnetizations as functions of K (Fig.3) are consistent with the physically expected behavior. As K increases, the impurity spin becomes gradually screened, while the magnetization of the nearest substrate spin decreases. Perfect singlet formation between $\vec{S}_0$ and $\vec{\sigma}$ is achieved only in the limit of infinitely large K. The behavior of the correlation functions (Fig.4) supports the above picture. The maximum value of 0.75 for the correlation function $C(\sigma, 0)$ is gradually approached with the increase of K. Notice that $< S_1^z >$ (Table.I) at any $K \neq 0$ is larger than the value at $K = 0$. This means that the quantum fluctuations have effectively decreased at that site. Such behavior was also observed in the 2D Heisenberg model with a missing site[3].

For small value of the Kondo coupling $K < 1$ our results for the magnetization are consistent with previous calculations of Igarashi, Murayama, and Fulde[9] in this regime, who used LSWA in combination with perturbation theory in K. We emphasize, however, that our calculation was specifically designed to treat the strong-coupling limit $K > 1$. Similar results to ours have been reported in the one-dimensional version of the model by Igarashi *et al.*[11]. They studied numerically the behavior of the quantities, defined in Eqs.(17-20). From comparison of our curves with theirs, we conclude that the tendency for local singlet formation is more pronounced for a Heisenberg chain, which is expected, since LRO is not present in 1D.

III. EXACT DIAGONALIZATION STUDIES.

We have also studied the system by exact diagonalization of small clusters. Traditionally periodic boundary conditions (PBC) are used[15]. However we have found in the study of related problems, involving locally frustrating spin defects[5] that the use of PBC may lead to spurious discontinuities in the observables. We have attributed this to finite size effects[6]. Instead, in our previous work[6] we applied a staggered magnetic field in the z direction to spins on the boundary of the cluster (see Fig.1). The same procedure is used here. We have chosen a cluster of $N = 18 + 1$ spins and the boundary field to give $< S^z >= 0.3$ on the boundary spins. The advantage of such an approach is that the sublattice symmetry is broken which allows us to compute single spin averages and to distinguish between longitudinal and transverse correlations. Our results are summarized in Table.I and Figures 3 and 4, for comparison with the analytic approach. Due to the asymmetry of the cluster the correlation function $C(1,0)$ is computed as $[C(1,0) + C(2,0) + C(3,0) + C(4,0)]/4$ (see Fig.1). Analogous symmetrization was used for $< S_1^z >$. We find a very good qualitative agreement between the analytical and exact diagonalization results.

Our numerical procedure also breaks the translational invariance of the cluster and will, in general, lead to increased finite size effects and slow convergence to the bulk limit. To achieve complete self-consistency, the extrapolation to the thermodynamic limit has to be performed, by adjusting simultaneously the boundary field to be equal to the magnetization of the spins inside the cluster. This certainly would increase even further the numerical agreement between the analytical and numerical results.

IV. SUMMARY AND DISCUSSION.

To summarize, we have studied the competition between LRO and local singlet formation in the 2D Heisenberg model at $T = 0$, coupled to a magnetic impurity via an on-site Kondo term. We were particularly interested in developing a formalism to treat large Kondo cou-

plings, since it is physically clear, that due the presence of LRO in 2D, only large couplings can lead to substantial impurity screening and local suppression of the magnetization. We find that the local singlet is formed asymptotically. At intermediate couplings the magnetization sustains a non-zero value, which gradually decreases as the coupling increases. This picture is supported by the two methods we have used: 1.) An analytic approach, which treats exactly the system, consisting of the impurity and the directly coupled to it host spin, and takes into account the interaction with the AFM background perturbatively, and 2.) Exact diagonalization of small clusters.

A related problem is the behavior of a Kondo moment in a system without LRO in the ground state (non-zero gap in the magnon energy spectrum). Destruction of LRO can be achieved e.g. by doping, or by introduction of additional spin interactions. The lack of LRO would lead to different behavior, compared to the one found in this paper, since the impurity could become completely screened at intermediate couplings. An interesting question is the existence of impurity induced bound states in the gap. Such states have been found in the $S = 1$ Heisenberg chain[16], and in s-wave (as well as d-wave under certain conditions) superconductors with magnetic impurities[17]. We plan to address these issues in future work.

ACKNOWLEDGMENTS

We would like to acknowledge the financial support of the Australian Research Council.

---

[1] See, e.g., E. Manousakis, Rev. Mod. Phys. **63**, 1 (1991).

[2] For a review, see E. Dagotto, Rev. Mod. Phys. **66**, 763 (1994).

[3] N. Bulut, D. Hone, D. J. Scalapino, and E. Y. Loh, Phys. Rev. Lett. **62**, 2192 (1989).

[4] N. Nagaosa, Y. Hatsugai, and M. Imada, J. Pys. Soc. Jpn. **58**, 978 (1989).

[5] J. Oitmaa, D. Betts, and M. Aydin, Phys. Rev. B **54**, 15171 (1995).

[6] V.N. Kotov, J. Oitmaa, and O. Sushkov, preprint cond-mat/9712281.

[7] K. Lee and P. Schlottmann, Phys. Rev. B **42**, 4226 (1990).

[8] S. Eggert and I. Affleck, Phys. Rev. B **46**, 10866 (1992); D. G. Clarke, T. Giamarchi, and B. I. Shraiman, Phys. Rev. B **48**, 7070 (1993).

[9] J. Igarashi, K. Murayama, and P. Fulde, Phys. Rev. B **52**, 15966 (1995).

[10] K. Murayama and J. Igarashi, J. Phys. Soc. Jpn. **66**, 1157 (1997).

[11] J. Igarashi, T. Tonegawa, M. Kaburagi, and P. Fulde, Phys. Rev. B **51**, 5814 (1995); W. Zhang, J. Igarashi, and P. Fulde, Phys. Rev. B **54**, 15171 (1996).

[12] W. Zhang, J. Igarashi, and P. Fulde, J. Pys. Soc. Jpn. **66**, 1912 (1997).

[13] The absence of vertex corrections in this problem is analogous to the same effect in the t-J model[2], and follows from the form of the fermion - spin-wave vertex.

[14] For details of a similar calculation, involving three spins, see Ref.[6], where the problem of an external spin, coupled symmetrically to the two sublattices, is studied.

[15] J. Oitmaa and D. Betts, Can. J. Phys. B **56**, 897 (1978).

[16] E. Sorensen and I. Affleck, Phys. Rev. B **51**, 16115 (1995).

[17] For recent work and references, see M.I. Salkola, A.V. Balatsky, and J.R. Schrieffer, Phys. Rev. B **55**, 12648 (1997).

TABLE I. Magnetization on site 1 calculated by the Greeen's function (GF) technique and by exact diagnalization (ED) of N=18+1 cluster.

K	0	1	2	3	4	5
$\lvert < S_1^z > \rvert$(GF)	0.318	0.327	0.334	0.330	0.329	0.328
$\lvert < S_1^z > \rvert$(ED)	0.3717	0.3804	0.3822	0.3820	0.3814	0.3809

FIGURE CAPTIONS

FIG. 1. Schematic representation of the system. The black dots are the host spins, with interaction J=1 between them. A cell, containing N= 18 + 1 sites, used for exact diagonalization, is shown.

FIG. 2. One-loop diagrams, contributing to the two-particle Green's function, Eq.(9). Solid and dashed lines represent fermion and spin-wave Green's functions, respectively.

FIG. 3. The impurity spin average $M(\sigma)$ and the magnetization of the neighboring host spin $M(0)$. The solid and dashed curves are calculated from Eq.(17) and Eq.(18), while the circles and squares are the corresponding exact diagonalization results.

FIG. 4. Spin-spin correlation functions as defined by Eq.(19) and Eq.(20). The solid and dashed line are obtained by numerical evaluation of Eqs.(19-20). The open symbols are the corresponding exact diagonalization results.

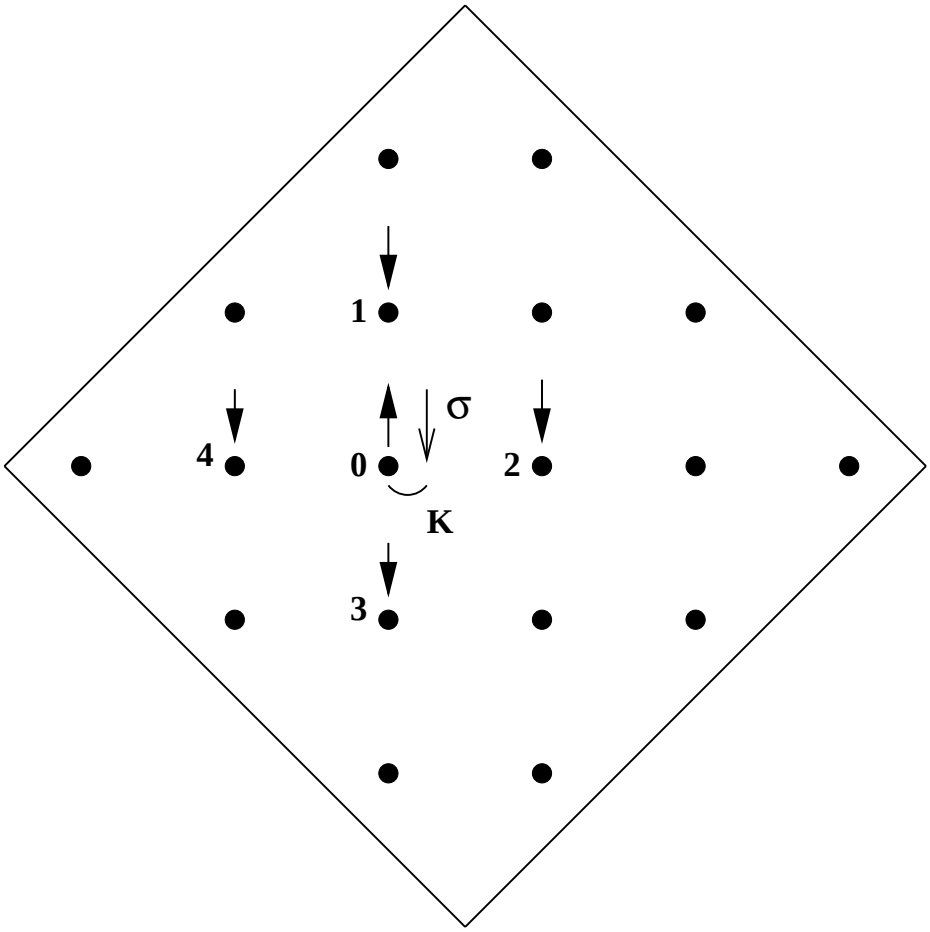

FIG.1.

(a)

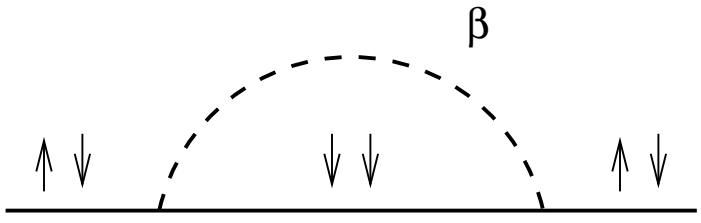

(b)

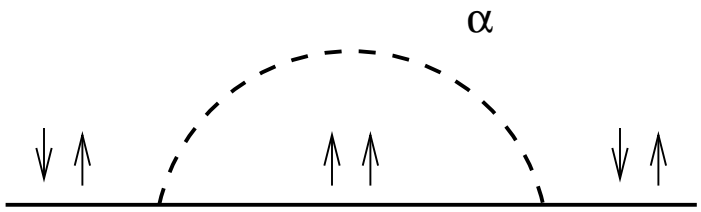

FIG.2.

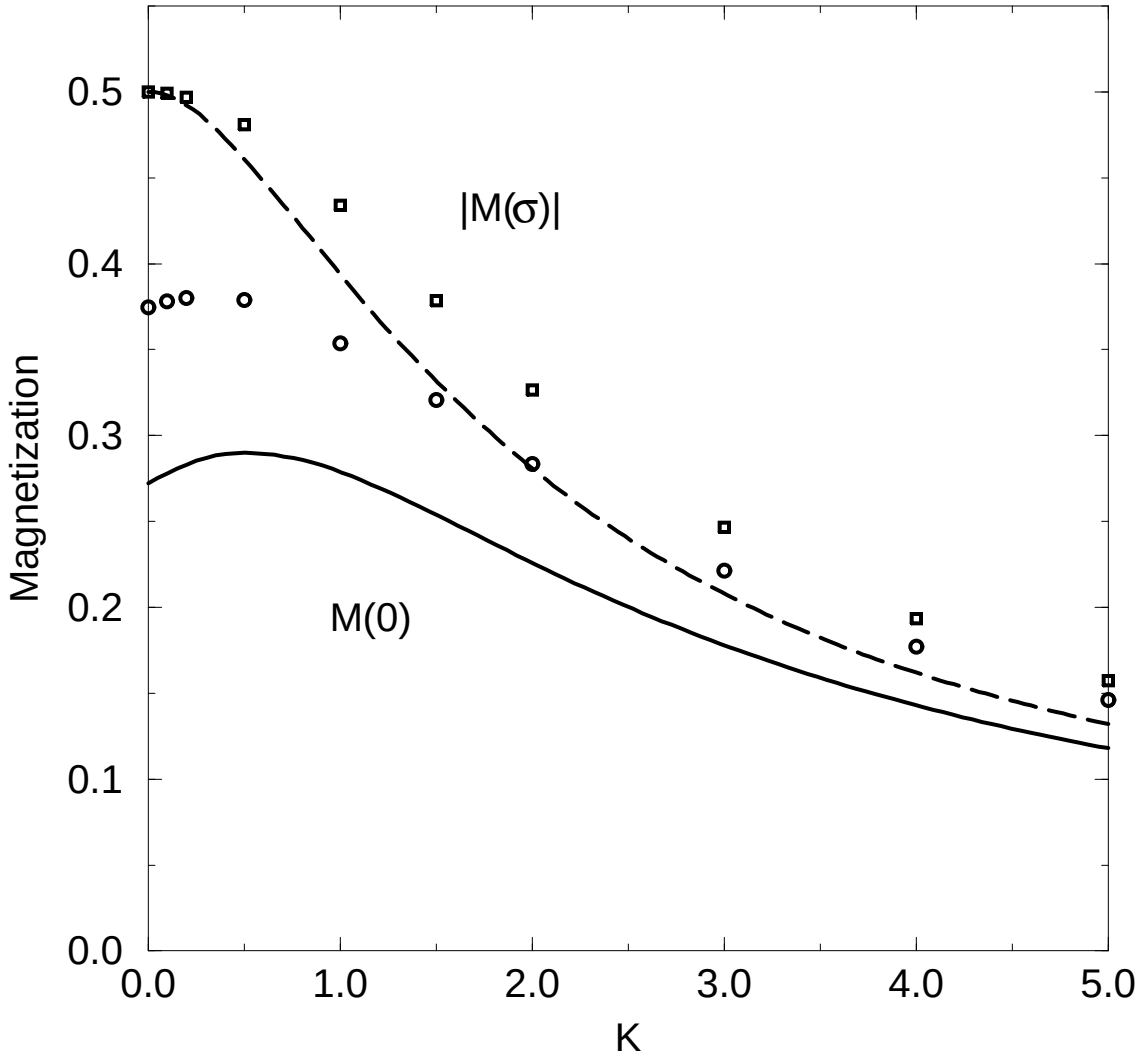

FIG.3.

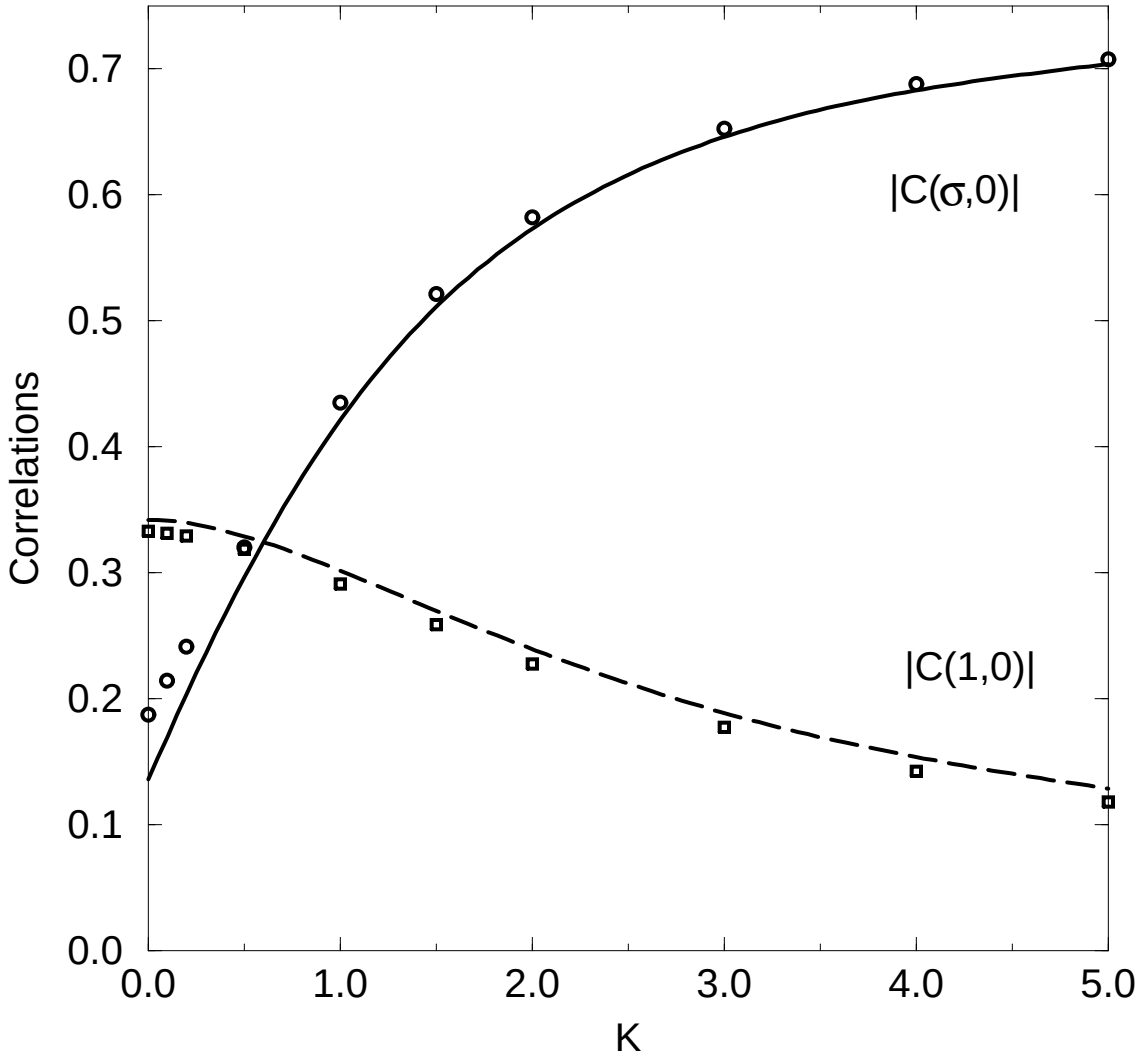

FIG.4.